ISSN 1070-4272, Russian Journal of Applied Chemistry, 2012, Vol. 85, No. 5, pp. 731–735. © Pleiades Publishing, Ltd., 2012.
Original Russian Text © L.N. Maskaeva, I.V. Zarubin, E.G. Vovkotrub, V.F. Markov, 2012, published in Zhurnal Prikladnoi Khimii, 2012, Vol. 85, No. 5, pp. 729–734.

INORGANIC SYNTHESIS AND INDUSTRIAL INORGANIC CHEMISTRY

Conditions of Hydrochemical Synthesis, Composition, and Structure of Tellurium Films

L. N. Maskaeva[a], I. V. Zarubin[a], E. G. Vovkotrub[b], and V. F. Markov[a]

[a] *Yeltsin Ural Federal University, Federal State Autonomous Educational Institution of Higher Professional Education, Yekaterinburg, Russia*
[b] *Institute of High-Temperature Electrochemistry, Ural Branch, Russian Academy of Sciences, Yekaterinburg, Russia*
e-mail: ivan-carevich85@mail.ru

Received April 18, 2011

Abstract—Conditions of the hydrochemical synthesis of thin tellurium films by reduction of an aqueous solution of tellurous acid with hydrazine were determined. The redox potentials of tellurous acid and hydrazine and their difference in relation to pH of the medium and concentration of tellurite ions were calculated. The kinetics of tellurium layer growth on glass-ceramic substrates and the structure, composition, and morphology of the layers were studied.

DOI: 10.1134/S1070427212050084

Thin tellurium films are widely used for optical information recording, in γ-radiation detectors, and for fabrication of solar batteries and field-effect transistors [1, 2]. There is no common opinion on the structure of tellurium films. Some authors prove that tellurium can exist only in the crystalline form [3], whereas other authors admit the existence of amorphous tellurium [4]. The specificity of the structure is responsible for the dependence of many electrophysical properties of tellurium on the voltage applied. Various methods for preparing elemental tellurium films have been described [3]: sublimation, distillation, thermal vacuum deposition, and molecular-beam epitaxy; particles of hexagonal tellurium can also be grown using microorganisms [5]. However, preparation of the high-quality material remains an intricate program.

A promising method for preparing tellurium, taking into account its colloid-chemical nature, is hydrochemical deposition. The method does not require sophisticated equipment, is simple in implementation, and allows the conditions of low-temperature synthesis to be widely varied. However, implementation of this method requires knowledge of the conditions under which elemental tellurium is formed in the reaction mixture. Previously published data on the deposition of elemental tellurium and tellurides are restricted only to various formulations of deposition baths [6, 7]. Data on the chemical mechanism of processes leading to the tellurium formation are scarce and contradictory [8].

The goal of this study was to examine regular trends in reduction of Te^{IV} compounds to Te^0 with hydrazine, to predict the conditions of the hydrochemical synthesis of nanostructured tellurium films, and to determine the composition, structure, and electrophysical properties of the films.

EXPERIMENTAL

The investigation objects were tellurium films prepared by the hydrochemical procedure from reaction mixtures containing potassium tellurite using a solution of hydrazine hydrochloride as reductant. The pH was adjusted with alkali or nitric acid and was monitored with a pH meter. As substrates we used 30 × 24 mm plates of ST-150-1 grade glass-ceramic. The substrates were degreased with a hot (323–343 K) solution of chromic mixture and etched in dilute (1 : 20) hydrofluoric acid.

Then the substrates were placed in a molybdenum glass reactor. The reactor was arranged in a U-10 thermostat. The temperature was maintained with an accuracy of ±0.1 K. In all the experiments, the reactants were added in a strictly definite order.

The synthesized tellurium films were heat-treated in air in a PM-1.0-7 electric furnace at 593 K. The temperature in the zone of the specimen arrangement was maintained with an accuracy of ±2 K. The furnace with tellurium film specimens placed in it was heated to the required temperature and then switched off and allowed to slowly cool to room temperature. The working temperature was attained, on the average, within 15–20 min, and the cooling lasted for 12–14 h.

X-ray diffraction studies were performed with a DRON-UM1 diffractometer using CuK_α radiation (λ = 1.15418 Å) at room temperature in the 2θ range 20°–80° in the step-by-step scanning mode with 0.04° step and 10-s signal accumulation in each step. The structural parameters of the synthesized tellurium films were refined by the Rietveld method of full-profile analysis using FULLPROF program [9].

The film composition was examined by laser Raman spectroscopy. Studies were performed with an InVi, Renishaw-1000 Raman microspectrometer. The spectra were recorded with a Mole microprobe analyzer (argon laser with a power of up to 600 mW, λ = 514.5 nm). Electron microscopic images of tellurium films were taken with a JEOL JSM-5900 LV scanning electron microscope.

Photoelectric properties of tellurium films were studied in accordance with GOST (State Standard) 17782–79 using a K 54.410 measurement installation.

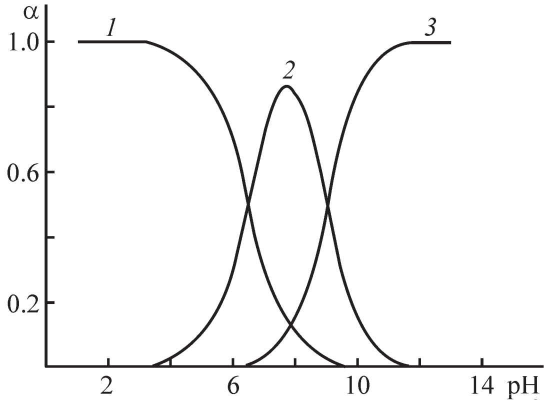

Fig. 1. Influence of pH on tellurous acid speciation. (α) Fraction of species. (*1*) H_2TeO_3, (*2*) $HTeO_3^-$, and (*3*) TeO_3^{2-}.

The hydrochemical synthesis of tellurium films is based on reduction of tellurite ions to elemental tellurium. Tellurous acid in aqueous solution dissociates to form $HTeO^-$ and TeO_3^{2-} ions (pk'_{Te} = 6.29, pk''_{Te} = 9.43) [10].

The analytical concentration of tellurium in solution is equal to the sum of the concentrations of its species: $c_{Te} = [H_2TeO_3] + [HTeO_3^-] + [TeO_3^{2-}]$.

The fraction of each species depends on pH and can be calculated from the ionic equilibria. The tellurous acid speciation in relation to pH is shown in Fig. 1.

The solubility of tellurous acid is strongly influenced by pH. In aqueous solutions at pH from 0.7 to 8.7, a voluminous white precipitate of tellurium(IV) oxide $TeO_2{\cdot}nH_2O$ is formed, which affects the Te^{IV} concentration in solution. Therefore, when calculating the pH dependence of the concentrations of various tellurous acid species, it is necessary to take into account data on the solubility of tellurium(IV) oxide. According to [11], the solubility of $TeO_2{\cdot}nH_2O$ is minimal at pH from 4 to 5. The pH dependence of the Te^{IV} concentration, taking into account the $TeO_2{\cdot}nH_2O$ solubility, is shown in Fig. 2.

Among reagents capable to reduce tellurous acid to Te^0, hydrazine is advantageous in that its use practically excludes contamination of the films with decomposition products. Aqueous solutions of hydrazine exhibit basic properties. Hydrazine is predominantly a monoacidic base [12, 13] forming the $N_2H_5^+$ ion in acid solutions. The total concentration of hydrazine c_h in solution can be expressed as $c_h = [N_2H_5^+] + [N_2H_4]$. The fraction of each hydrazine species also depends on pH. The hydrazine speciation in relation to pH is shown in Fig. 3. As seen from Fig. 3, at pH 5–10 both hydrazine species coexist in the solution.

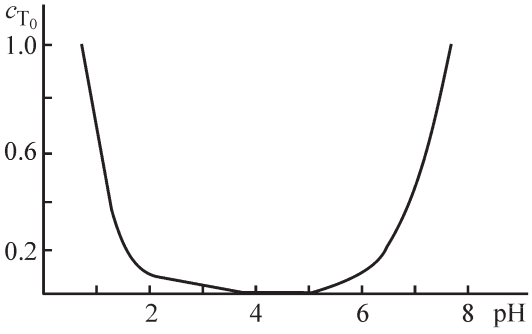

Fig. 2. Influence of pH on the relative content c_{Te} of soluble Te species.

In our study we considered two schemes of Te^{IV} reduction with hydrazine in acid and alkaline solutions, i.e., the reactions involving molecular and ionic hydrazine species. The Te^{IV} reduction to Te^0 can be described by the equations

$$TeO_3^{2-} + H^+ + N_2H_5^+ = N_2\uparrow + Te\downarrow + 3H_2O\ ,$$
$$TeO_3^{2-} + N_2H_4 = Te\downarrow + N_2\uparrow + H_2O + 2OH^-\ .$$

The possibility of the occurrence of a redox reaction can be judged from the emf, which depends on the reactant concentrations, pH, temperature, and other factors. The difference between the redox potentials φ_{N_2/N_2H_4} and $\varphi_{Te/TeO_3^{2-}}$ depends on pH and concentration of tellurite ions as follows:

$$\varphi_{Te/TeO_3^{2-}} - \varphi_{N_2/N_2H_4} = 0.278 - 0.03pH + 0.0151\log\,[TeO_3^{2-}].$$

The results of calculating the potentials of hydrazine and of tellurite ions and the potential difference for this couple are shown in Fig. 4. Thermodynamic analysis shows that the Te^{IV} reduction with hydrazine to Te^0 is possible in the entire pH range. The emf of the reduction reactions is positive and varies from 0.486 to 0.676 V. The dependence has a maximum at pH 9. Hence, deposition of elemental Te from aqueous solutions with hydrazine is most probable in alkaline solutions. Taking into account the parameters affecting the film thickness, we obtained the optimal composition of the reaction mixture: $[TeO_3^{2-}] = 2 \times 10^{-2}$ M, $[N_2H_4{\cdot}2HCl] = 1$ M.

The hydrochemical synthesis from alkaline tellurite solutions allowed us to prepare 240 to 300 nm thick elemental tellurium layers on glass-ceramic substrates. The tellurium layers synthesized from this composition were examined by X-ray phase analysis, electron microscopy, and laser Raman spectroscopy.

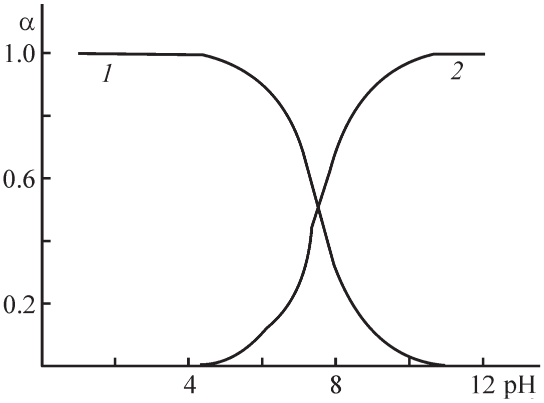

Fig. 3. Influence of pH on the fraction α of molecular and ionic hydrazine species. (*1*) $\alpha_{N_2H_5^+}$ and (*2*) $\alpha_{N_2H_4}$.

Figure 5 shows an X-ray diffraction pattern of a Te film deposited from the reaction mixture of the above-given composition. In the X-ray diffraction pattern, we identified only the hexagonal structure of the A8 type, characteristics of tellurium, and reflections of the glass-ceramic substrate [main component: titanium(IV) oxide].

The interplanar spacings of the tellurium crystal lattice in the film prepared from the base composition are given in the table in comparison with the reference data. As can be seen, the interplanar spacings in the structure of the deposited tellurium films practically coincide with the reference data for the Te single crystal, suggesting high ordering of the crystal structure.

By the Rietveld method of full-profile analysis, using the FULLPROF program, we determined the unit cell parameters: $a = 0.44535$, $b = 0.44535$, $c = 0.59283$ nm. These values are well consistent with the reference data: $a = 0.4457$, $b = 0.4457$, $c = 0.59290$ nm [13]. The

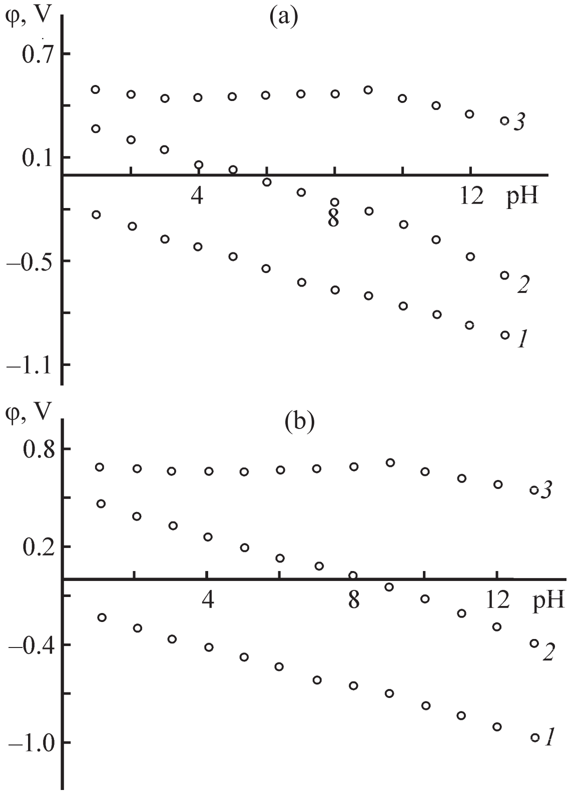

Fig. 4. Influence of pH on the potentials φ of (*1*) hydrazine, φ_{N_2/N_2H_4}, and (*2*) tellurite ions, $\varphi_{Te/TeO_3^{2-}}$, and on the (*3*) difference between them for the reactions involving (a) N_2H_4 and (b) $N_2H_5^+$.

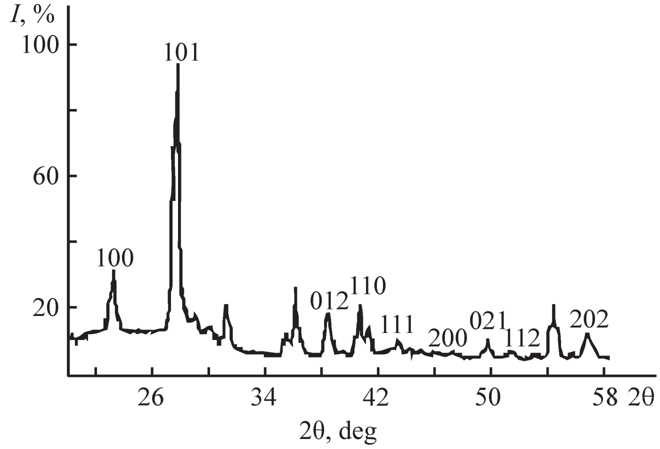

Fig. 5. X-ray diffraction pattern of a Te film. (*I*) Intensity and (2θ) Bragg angle.

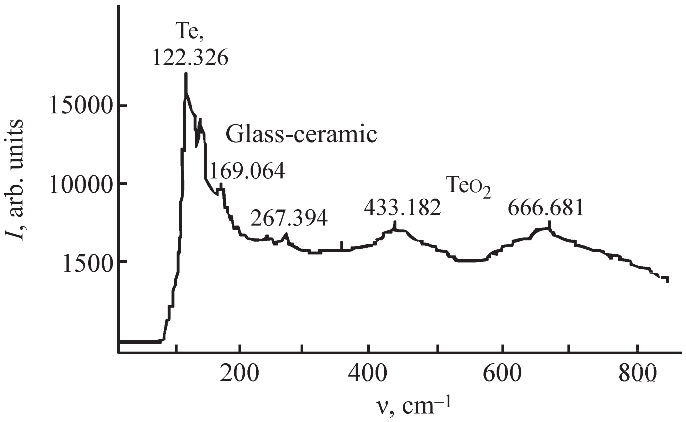

Fig. 6. Raman spectrum of a Te film freshly deposited from the reaction mixture of the base composition. Substrate: ST-150-1 glass-ceramic. (*I*) Intensity and (ν) wavenumber.

reflection half-width was 0.283.

The presence of elemental tellurium on the substrates is confirmed by the Raman spectra (Fig. 6) exhibiting peaks characteristic of the trigonal tellurium structure [14, 15]. The peaks at 441, 605, 169, and 243 cm^{-1} belong to the glass-ceramic substrates. At 667 and 433 cm^{-1}, there are smeared peaks belonging to tellurium(IV) oxide. The X-ray diffraction data for the films suggest that tellurium(IV) oxide present in them is X-ray amorphous.

The freshly deposited Te films are not photosensitive. For their sensitization, they were heat-treated at 593 K. After the annealing, the Te unit cell parameters were as follows: $a = 0.44945$, $b = 0.44945$, $c = 0.58862$ nm, i.e., the parameters a and b increased, whereas c decreased.

The reflections in the X-ray diffraction patterns of the heat-treated Te layers are considerably less intense and are appreciably broadened (0.350) relative to the freshly deposited films (0.283). The reflection broadening and an increase in the unit cell parameters may be due to the following facts: small size of coherent scattering domains (to a first approximation, small crystallite size) and appearance of stresses and microstrains in the specimen.

The results of electron-microscopic examination of

Interplanar spacings d of the Te crystal lattice for the film deposited from the reaction mixture of the base composition onto ST-150-1 glass-ceramic in comparison with ASTM data [10]

hkl	Reflection			
	ICDD reference data		our data	
	d_{hkl}, nm	2θ, deg	d_{hkl}, nm	2θ, deg
100	3.8600	23.022	3.8545	23.055
101	3.2349	27.551	3.2306	27.588
012	2.3511	38.250	2.3435	38.378
100	2.2286	40.442	2.2257	40.497
111	2.0861	43.339	2.0833	43.398
200	1.9300	47.046	1.9292	47.067
021	1.8352	49.635	1.8326	49.711
112	1.7814	51.242	1.7838	51.165
202	1.6174	56.881	1.6174	56.883

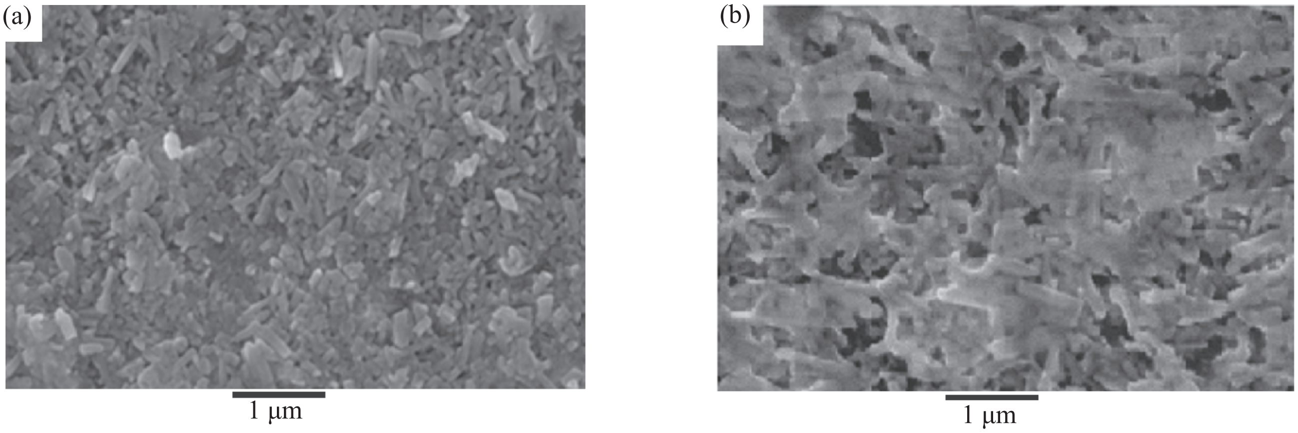

Fig. 7. Electron micrograps of a Te film, (a) freshly deposited and (b) heat-treated at 593 K.

the films obtained are of indubitable interest. Figure 7 shows the electron micrographs of the freshly deposited and heat-treated (593 K) Te films. Comparison of the images shows that the film morphology changes upon annealing. As can be seen, the freshly deposited film is formed of crystallites whose size does not exceed 100 nm. It should be noted that the Te microcrystals are well-faceted rectangular particles of length 0.2–0.5 and width 0.1–0.2 μm, fairly uniformly distributed on the substrate. The mean Te crystallite size increased upon annealing by a factor of ~2 owing to coarsening as a result of recrystallization.

The dark resistance of the Te film after the heat treatment increased from 35 to 1400 kΩ. The dark current and photocurrent of the heat-treated 300 nm thick Te film were 10×10^{-5} and 11.8×10^{-5} A, respectively. The ratio of the photocurrent to the dark current was about 2.

CONCLUSIONS

(1) Calculation of the redox potentials in the tellurous acid–hydrazine system at various pH values and tellurite ion concentrations shows that the reduction of tellurite ions is most probable in alkaline solutions.

(2) Elemental tellurium films 240 to 300 nm thick on glass-ceramic substrates were prepared for the first time by hydrochemical deposition.

(3) The unit cell parameters, composition, and morphology of the hydrochemically deposited elemental tellurium films were determined by X-ray phase diffraction, electron microscopy, and Raman spectroscopy.

(4) The chemically deposited Te layers heat-treated at 593 K exhibit photosensitivity to IR radiation.

REFERENCES

1. Goldobin, A.N. and Lezheiko, L.V., *Fiz. Tverd. Tela*, 1961, vol. 3, no. 10, pp. 3247–3249.
2. Slavnov, A.G., *Izv. Vyssh. Uchebn. Zaved., Fiz*., 1967, vol. 3, pp. 128–130.
3. Novoselova, A.V., *Redkie metally i ikh primenenie* (Rare Metals and Their Use), Moscow: Znanie, 1966.
4. Stishov, S.M. and Tikhomirova, N.A., *Zh. Eksp. Teor. Fiz*., 1965, vol. 4, no. 2, pp. 618–620.
5. Tucker, F. and Walper, J., *J. Bacteriol*., 1961, vol. 83, pp. 1313–1314.
6. Kulifay, S.M., *J. Am. Chem. Soc*., 1961, vol. 83, no. 24, p. 4916.
7. US Patent 3058802.
8. Belyaev, A.I. and Berchenko, M.A., *Zh. Neorg. Khim*., 1970, vol. 15, p. 2005.
9. Rietveld, H.M., *J. Appl. Crystallogr*., 1969, vol. 2, pp. 65–71.
10. Lur'e, Yu.Yu., *Spravochnik po analiticheskoi khimii* (Handbook of Analytical Chemistry), Moscow: Khimiya, 1971.
11. Cheng, K.L., *Anal. Chem.,* 1961, vol. 33, no. 6, pp. 761–764.
12. Audrieth, L.F. and Ogg, B.A., *The Chemistry of Hydrazine*, New York: Wiley, 1951.
13. *ASTM X-ray Diffraction Data Cards*, Philadelphia, 1968, no. 6–0354.
14. Artamonov, V.V., Baidullaeva, A., and Vlasenko, A.I., *Fiz. Tverd. Tela*, 2004, vol. 46, no. 8, pp. 1489–1493.
15. Belogorokhov, A.I., Denisov, I.A., and Smirnova, N.A., *Fiz. Tekh. Poluprovodn*., 2004, vol. 38, no. 1, pp. 84–93.